tvst

Article

Visualization of the Retina in Intact Eyes of Mice and Ferrets Using a Tissue Clearing Method

Yunyan Ye[1,2], Tung Anh Dinh Duong[1,3], Kengo Saito[1], Yohei Shinmyo[1], Yoshie Ichikawa[1], Tomomi Higashide[2], Kyosuke Kagami[4], Hiroshi Fujiwara[4], Kazuhisa Sugiyama[2], and Hiroshi Kawasaki[1]

[1] Department of Medical Neuroscience, Graduate School of Medical Sciences, Kanazawa University, Ishikawa, Japan
[2] Department of Ophthalmology, Graduate School of Medical Sciences, Kanazawa University, Ishikawa, Japan
[3] Pediatrics Department, Hai Phong University of Medicine and Pharmacy, Hai Phong, Vietnam
[4] Department of Obstetrics and Gynecology, Graduate School of Medical Sciences, Kanazawa University, Ishikawa, Japan

Correspondence: Kazuhisa Sugiyama, Department of Ophthalmology, Graduate School of Medical Sciences, Kanazawa University, Takara-machi 13-1, Kanazawa, Ishikawa 920-8640, Japan. e-mail: ksugi@med.kanazawa-u.ac.jp Hiroshi Kawasaki, Department of Medical Neuroscience, Graduate School of Medical Sciences, Kanazawa University, Takara-machi 13-1, Kanazawa, Ishikawa 920-8640, Japan. e-mail: hiroshi-kawasaki@umin.ac.jp

Received: June 10, 2019
Accepted: November 14, 2019
Published: February 7, 2020

Keywords: CUBIC; immunostaining; intact eye; melanin bleach; retina

Citation: Ye Y, Dinh Duong TA, Saito K, Shinmyo Y, Ichikawa Y, Higashide T, Kagami K, Fujiwara H, Sugiyama K, Kawasaki H. Visualization of the retina in intact eyes of mice and ferrets using a tissue clearing method. Trans Vis Sci Tech. 2020;9(3):1, https://doi.org/10.1167/tvst.9.3.1

Purpose: Visualization of specific cells and structures in intact organs would greatly facilitate our knowledge about pathological changes; therefore, a tissue clearing method applicable to the intact eye may be valuable. Here we report a novel imaging method for the retina using the hyperhydration-based tissue clearing technique CUBIC (Clear, Unobstructed Brain/Body Imaging Cocktails and Computational Analysis).

Methods: Eyes of Institute of Cancer Research (ICR) mice, C57BL/6 mice, and normally pigmented sable ferrets (*Mustela putorius furo*) were used. Intact eyes were subjected to CUBIC, melanin bleaching with H_2O_2, and immunostaining. Images of the retina in intact eyes were taken using epifluorescence microscopes and confocal microscopes.

Results: The combination of melanin bleaching and CUBIC efficiently made the eyes of C57BL/6 mice transparent. By combining melanin bleaching, CUBIC, and immunostaining, we succeeded in visualization of retinal structures from the outside of the intact eyes of mice. Furthermore, we found that our methods were applicable not only to mouse eyes but also to ferret eyes, which are much larger than those of mice.

Conclusions: Our method was useful for visualizing specific cells and structures in the retina of intact eyes with single-cell resolution without making tissue sections.

Translational Relevance: This simple and efficient method can be applicable to various rodent models, including those associated with glaucoma or myopia, and will facilitate evaluating the effects of novel therapy for relevant eye diseases by visualizing changes from the retina to the sclera at both molecular and macroscopic levels simultaneously in a whole-eye preparation.

Introduction

The eye is a crucial organ for visual perception. After entering through the pupil and the lens, visual information from the outside world is detected by the retina. Neuronal activity generated in the retina is transmitted through the optic nerve to the visual system in the brain. The retina contains not only various types of neurons such as retinal ganglion cells

(RGCs) but also retinal pigmented epithelial cells and microglia, all of which are important for the physiological functions of the retina. These cells in the retina are often damaged and involved in pathological conditions; for example, RGCs are degenerated in glaucoma patients, and microglia are activated in response to inflammation and infection in the eye.[1–3] Molecular and histological analyses of the retina are crucial for understanding the functions and pathophysiology of the retina.

Previously, many studies performed molecular and histological analyses of the eye using classical tissue sections and histological techniques. Although these classical techniques are useful for analyzing fine structures within tissue sections, images of the whole retina are difficult to obtain. Furthermore, because the retina is thin and fragile, it is often difficult to maintain the morphology and structures of the native retina during cutting and staining. Another technique used for the retina is immunostaining using isolated free-floating retinas. The whole retina isolated from the eye can be stained with antibodies and dyes. This staining using isolated free-floating retinas provides not only structural information about the retinal layers but also spatial information about the whole retina. On the other hand, however, retinal pigmented epithelium and the peripheral retina are lost during preparation of isolated free-floating retinas; therefore, it would be desirable to have a novel analytical technique to investigate the intact eye.

Recently, several pioneering studies have reported tissue clearing methods such as Sca*l*e, SeeDB, CLARITY, 3DISCO, ClearT, and CUBIC,[4–9] which have enabled acquiring images of the whole organs without making tissue slices. These methods have been used mainly for brains, but they are also useful for other organs,[10–15] providing fundamental information for understanding the functional and pathophysiological mechanisms. For this reason, we thought it would be valuable if a tissue clearing method could be applied to the intact eye; however, it has been difficult to apply tissue clearing methods to the eye, mainly because the eye contains abundant melanin in the retinal pigmented epithelium and the uvea. Indeed, the eye remains black even after treatment with many of the tissue clearing methods.[16] By combining the tissue clearing method CUBIC, melanin bleaching, and immunostaining, we succeeded in making the eye transparent and acquiring images of the retina from outside of the eye without making sections. Our procedure will significantly contribute to uncovering the functions of the eye and the pathophysiological mechanisms of its diseases.

Materials and Methods

Animals

Institute of Cancer Research (ICR) mice and C57BL/6J mice were purchased from SLC (Hamamatsu, Japan). Normally pigmented sable ferrets (*Mustela putorius furo*) were purchased from Marshall Farms (North Rose, NY) and maintained as described previously.[17–19] All procedures were approved by the Animal Care Committee of Kanazawa University. All animals were treated in accordance with the Association for Research in Vision and Ophthalmology Statement for the Use of Animals in Ophthalmic and Vision Research. All experiments were performed at least three times and gave consistent results.

CUBIC Reagents

CUBIC reagents were prepared just prior to use. Before Triton X-100 (Sigma-Aldrich; St. Louis, MO) was added, all other chemicals were dissolved with a hot stirrer at 60°C. Because water evaporation makes it difficult for highly concentrated chemicals to be dissolved, the weight of the solution was monitored frequently, and distilled water was added during a mixing step. After all chemicals except Triton X-100 were dissolved, the solution was cooled to room temperature, and finally Triton X-100 was added.[9,14]

CUBIC-1 reagent contains 25% (w/w) urea (Nacalai Tesque, Inc.; Kyoto, Japan), 25% (w/v) N,N,N′,N′-tetrakis (2-hydroxypropyl) ethylenediamine (Tokyo Chemical Industry; Tokyo, Japan), and 15% (w/v) polyethylene glycol mono-*p*-isooctylphenyl ether (Triton X-100). CUBIC-2 reagent was prepared as a mixture of 50% sucrose (Nacalai Tesque), 25% (w/v) urea, 10% (w/v) 2,20,20′-nitrilotriethanol (Wako Pure Chemical Industries, Ltd.; Osaka, Japan), and 0.1% (v/v) Triton X-100.

Immunostaining Using Free-Floating Retinas

Immunostaining using free-floating retinas was performed as described previously with modifications.[20] After mice were deeply anesthetized, the eyes were dissected and fixed with 4% paraformaldehyde (PFA) in phosphate-buffered saline (PBS) at 4°C overnight. In each eye, the edge of the cornea was pierced with sharp scissors. An incision was made along the limbus, and the cornea was discarded. The lens and the vitreous humor were removed. The cup-shaped

retina was isolated and washed with PBS. Four to five radial incisions reaching approximately 2/3 of the radius of the retina were made using scissors to create a petal-shaped retina.

For immunostaining, retinas were incubated with blocking solution (0.5% Triton-X 100, 2% bovine serum albumin) for 2 hours at room temperature followed by incubation in primary antibodies overnight at 4°C. The primary antibodies used here were mouse Tuj1 (Covance; Princeton, NJ) and rabbit anti-Iba1 (Wako Pure Chemical Industries) antibodies. After being washed with 0.5% Triton X-100/PBS three times for 10 minutes each, retinas were incubated with secondary antibodies plus either Hoechst 33342 or propidium iodide (Life Technologies; Carlsbad, CA) for 4 hours at room temperature. Retinas were washed in 0.5% Triton X-100/PBS three times for 10 minutes each and mounted on slides. Images of the retinas were taken using a confocal microscope or an epifluorescence microscope.

Intact Eye Staining

Mice were deeply anesthetized and transcardially perfused with 4% PFA/PBS. Eyes were isolated and post-fixed with 4% PFA/PBS overnight at 4°C. The pigmented eyes were immersed in 10% H_2O_2/PBS for 3 hours at 55°C to bleach the melanin.[21] The eyes were washed with 0.5% Triton X-100/PBS three times for 10 minutes each at room temperature.

CUBIC tissue clearing and immunostaining were then performed as described previously with modifications.[9,14] The eyes were immersed in CUBIC-1 reagent at room temperature for 1 day with gentle shaking. After being washed with PBS three times for 10 minutes each with gentle shaking at room temperature, the eyes were immersed in 20% sucrose/PBS at 4°C overnight. The eyes were put in optimal cutting temperature (OCT) compound (Sakura Finetek; Tokyo, Japan) and frozen at –80°C for 24 hours. The frozen eyes were thawed and washed with PBS at 37°C three times for 10 minutes each. The efficiencies of tissue clearing and antibody penetration increased significantly after the eyes were frozen in OCT compound at –80°C overnight and thawed with PBS at 37°C.

After unnecessary fat tissue around each eye was removed using forceps and scissors, two small holes were made at the ora serrata using a 29-gauge needle. These two holes were located approximately 180° apart from each other. One hole was used for injection and the other for drainage. After block solution (0.1% Triton X-100, 0.5% bovine serum albumin, 0.01% sodium azide in PBS) was injected into the vitreous humor through a hole, the eyes were incubated in the blocking solution with gentle shaking for 4 hours at room temperature. The same intravitreal injection procedure was used in the subsequent processes. About 50 µl and 100 µl of antibody solutions were injected into the mouse eyes and the ferret eyes, respectively. The eyes were treated with primary antibodies, including anti-Iba1 (Wako Pure Chemical Industries), anti-Brn3a (Chemicon International; Temecula, CA), anti-CD31 (BD Pharmingen; San Jose, CA), and Tuj1 (Covance) antibodies, for 3 days at room temperature and washed with 0.5% Triton X-100/PBS three times for 10 minutes each. After the eyes were treated with secondary antibodies plus either propidium iodide or Hoechst 33342 for 1 day at room temperature with gentle shaking, the eyes were washed with 0.5% Triton X-100/PBS three times for 10 minutes each. The eyes were immersed in 20% sucrose/PBS overnight and in CUBIC-2 reagent for 2 days at room temperature.

When necessary, cup-shaped retinas were isolated, and four to five radial incisions reaching approximately 2/3 of the radius of each retina were made using scissors to create a petal shape. The retinas were mounted on slides, and images of the retinas were taken using a confocal microscope.

Imaging of Flat-Mounted Retinas and Stained Eyeballs

The images of flat-mounted retinas and stained intact eyes were taken using a BZ-9000 fluorescence microscope (Keyence; Osaka, Japan) and a confocal microscope (Carl Zeiss; Jena, Germany). The stained intact eye could be stably placed on slides because the CUBIC-2 reagent contains 50% sucrose.

Results

Tissue Clearing and Melanin Bleaching Using Intact Eyes

First, we applied CUBIC to the eyeballs of albino ICR adult mice and pigmented C57BL/6J adult mice. After cardiac perfusion with 4% PFA was performed, the eyes were dissected and incubated in CUBIC-1 reagent to remove lipids, then in 20% sucrose, and finally in CUBIC-2 reagent to reduce the refractive index (Fig. 1A, Table 1). We found that the eyes of ICR mice became markedly transparent (Fig. 1B), suggesting that CUBIC is suitable for making the sclera and the optic nerve transparent. In contrast, however,

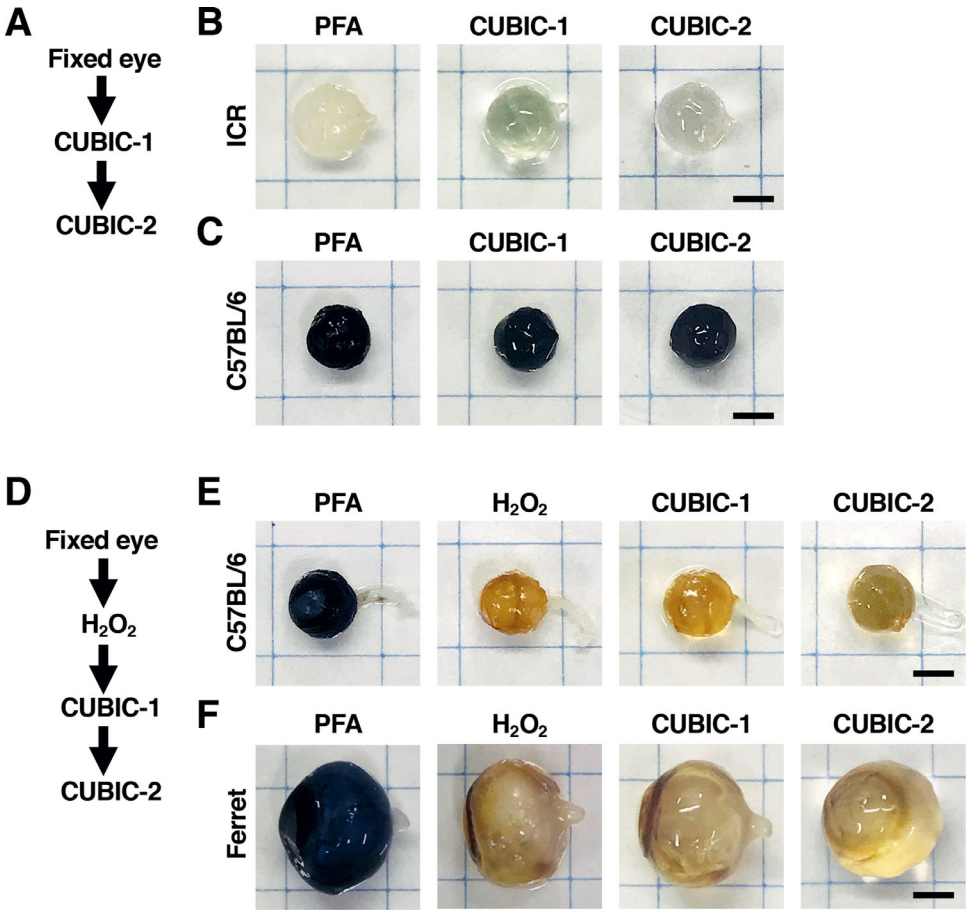

Figure 1. CUBIC and melanin bleaching of the eyes of adult mice and ferrets. (A) Experimental procedure for CUBIC used in (B) and (C); see Table 1 for details. (B) Brightfield images of the eyes of ICR mice after PFA, CUBIC-1, and CUBIC-2 treatment. The eyes of ICR mice became transparent after CUBIC treatment. (C) Brightfield images of the eyes of C57BL/6 mice after PFA, CUBIC-1, and CUBIC-2 treatment. The eyes of C57BL/6 mice did not become transparent even after CUBIC treatment because of melanin in the uvea and the retinal pigmented epithelium. (D) Experimental procedure for CUBIC combined with melanin bleaching used in (E) and (F); see Table 2 for details. (E) Brightfield images of the eyes of C57BL/6 mice after PFA, H_2O_2, CUBIC-1, and CUBIC-2 treatment. (F) Brightfield images of ferret eyes after PFA, H_2O_2, CUBIC-1, and CUBIC-2 treatment. Note that the combination of H_2O_2 and CUBIC treatment efficiently made the mouse eye and the ferret eye transparent. Scale bars, 20 mm.

Table 1. Detailed experimental procedure for Figures 1A–C

Day	Procedure
1	Cardiac perfusion with 4% PFA Isolation of the eye Post-fixation in 4% PFA at 4°C overnight
2	Washing with PBS, 10 min × 3 CUBIC-1 at RT for 1 d
3	Washing with PBS, 10 min × 3 20% sucrose at 4°C overnight
4	CUBIC-2 at RT for 2 d

RT, room temperature.

Table 2. Detailed experimental procedure for Figures 1D–F

Day	Procedure
1	Cardiac perfusion with 4% PFA Isolation of the eye Post-fixation in 4% PFA at 4°C overnight
2	Washing with PBS, 10 min × 3 Bleaching with 10% H_2O_2 for 3 h at 55°C Washing with PBS, 10 min × 3 CUBIC-1 at RT for 1 d
3	Washing with PBS, 10 min × 3 20% sucrose at 4°C overnight
4	CUBIC-2 at RT for 2 d

RT, room temperature.

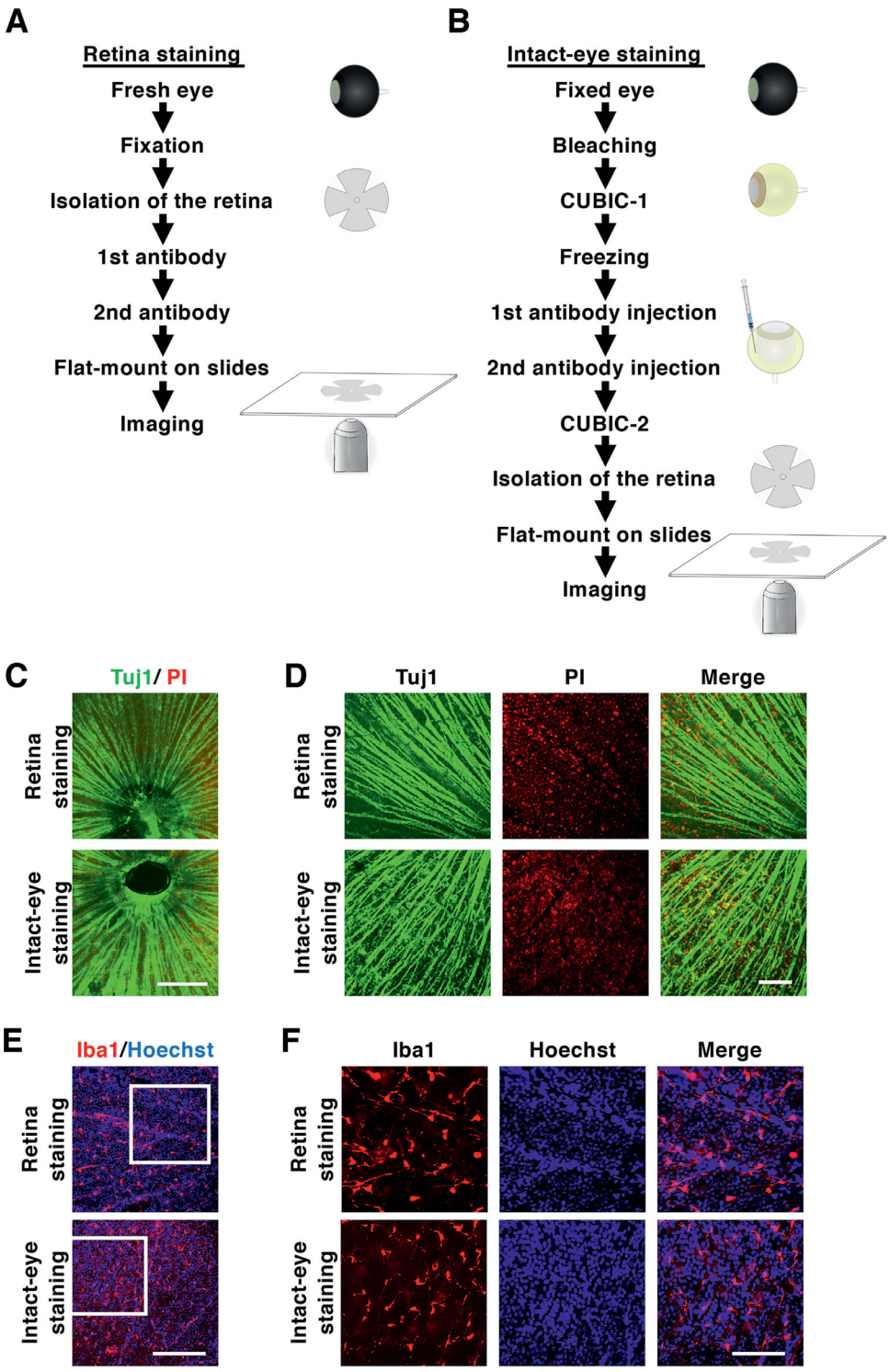

Figure 2. Comparison of immunostaining using isolated free-floating retinas and intact eyes. (A) Experimental procedure for immunostaining using isolated free-floating retinas; see Table 3 for details. (B) Experimental procedure for immunostaining using intact eyes; see Table 4 for details. After staining, the retina was isolated from the eye, and the flat-mounted retina was used to take images. (C, D) Tuj1 immunostaining using an isolated free-floating retina (upper) and an intact eye (lower) of C57BL/6 mice. Note that RGC axons were clearly stained with Tuj1 antibody in both cases. (E, F) Iba1 immunostaining using an isolated free-floating retina (upper) and an intact eye (lower) of ICR mice without CUBIC and melanin bleaching. Note that microglia were clearly stained with anti-Iba1 antibody in both cases. Scale bars, 200 µm (C, E) and 100 µm (D, F).

Table 3. Detailed experimental procedure for the retina staining in Figure 2A

Day	Procedure
1	Isolation of the eye
	Fixation in 4% PFA at 4°C overnight
2	Washing with PBS, 10 min × 3
	Isolation and preparation of the free-floating retina
	Blocking with 0.5% Triton X-100 and 2% BSA for 2 h
	Incubation with first antibody at 4°C overnight
3	Washing with PBST, 10 min × 3
	Incubation with second antibody at RT for 4 h
	Washing with PBST, 10 min × 3
	Flat-mounting on slides
	Imaging using a microscope

BSA, bovine serum albumin; PBST, 0.5% Triton X-100/PBS; RT, room temperature.

Table 4. Detailed experimental procedure for the intact-eye staining in Figure 2B

Day	Procedure
1	Cardiac perfusion with 4% PFA
	Isolation of the eye
	Post-fixation in 4% PFA at 4°C overnight
2	Washing with PBS, 10 min × 3
	Bleaching with 10% H_2O_2 for 3 h at 55°C
	Washing with PBS, 10 min × 3
	CUBIC-1 at RT for 1 d
3	Washing with PBS, 10 min × 3
	20% sucrose at 4°C for 1 d
	Freezing in OCT at –80°C overnight
4	Washing with PBS, 10 min × 3
	Blocking with 0.1% Triton X-100, 0.5% BSA at RT for 4 h
	First antibody injection and incubation at RT for 3 d
7	Washing with PBST, 10 min × 3
	2nd antibody injection and incubation at RT for 1 d
8	Washing with PBST, 10 min × 3
	20% sucrose at 4°C for 1 d
9	CUBIC-2 at RT for 2 d
11	Isolation and preparation of the petal-shaped retina
	Flat-mounting on slides
	Imaging using a microscope

BSA, bovine serum albumin; PBST, 0.5% Triton X-100/PBS; RT, room temperature.

consistent with previous studies, the eyes of C57BL/6J mice remained black (Fig. 1C), presumably because melanin is abundantly distributed in the uvea and the retinal pigmented epithelium of C57BL/6J mice.[16]

Previously, it was reported that the treatment of the retinal pigmented epithelium and choroidal melanocytes with H_2O_2 eliminated black color efficiently.[21] We therefore hypothesized that treatment of eyes with H_2O_2 and CUBIC would make the eyes of C57BL/6J mice transparent. We tried several concentrations, incubation times, and temperatures for the H_2O_2 treatment and found that 10% H_2O_2 at 55°C for 3 hours was optimum for eliminating black color from intact eyes of C57BL/6J mice (Figs. 1D, 1E; Table 2). Temperatures higher than 55°C and incubation times longer than 3 hours resulted in destruction of the eye, and lower temperatures and shorter incubation times were not enough to eliminate the black color. We found that the combination of H_2O_2 and CUBIC efficiently made the eyes of C57BL/6J mice transparent (Fig. 1E).

We further examined whether our method of combining H_2O_2 and CUBIC is also applicable to larger eyes. We used carnivore ferret eyes and found that the same method efficiently made ferret eyes transparent (Fig. 1F), suggesting that our method is useful for the eyes of various kinds of animals. In addition, it has been reported that various kinds of tissue clearing methods affect the sizes of treated tissues and, as a result, treated tissues are deformed.[22] It should be noted that the sizes of the eyeballs of mice and ferrets apparently were not affected by our method.

Intact Eye Immunostaining after Tissue Clearing and Melanin Bleaching

Having made intact mouse and ferret eyes transparent with H_2O_2 and CUBIC treatment, we next examined whether immunological detection could be performed using the transparent eyes. After H_2O_2 and CUBIC treatment, we first incubated the eyes in antibody solutions. After the entire immunostaining procedure, retinas were isolated and flat-mounted on slides. However, signals were not observed in the flat-mounted retinas, presumably because antibody cannot penetrate the eye through the sclera.

We therefore made small holes at the ora serrata and injected a solution containing Tuj1 antibody directly into the vitreous humor through the hole following

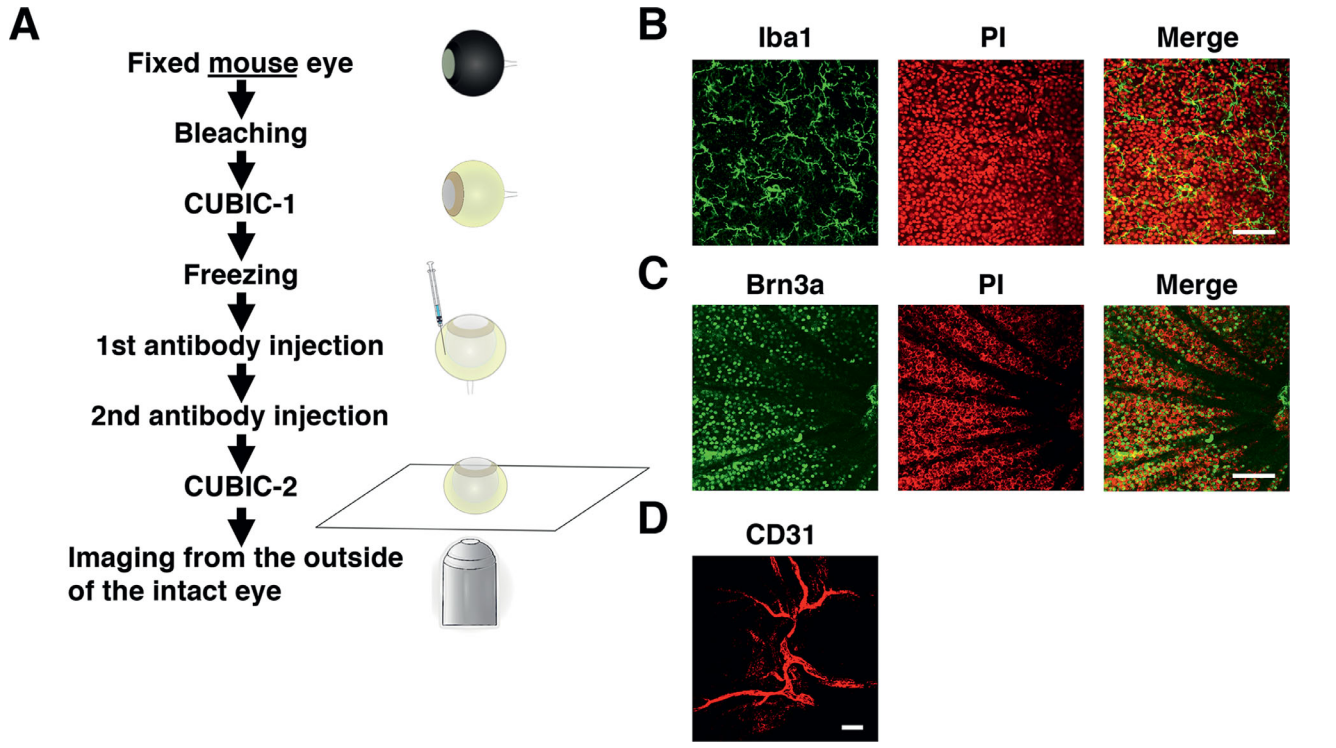

Figure 3. Imaging of the retina in intact mouse eyes from the outside of the eye. (A) Experimental procedure. After immunostaining using intact mouse eyes, images were taken from the outside of the eye without making sections using confocal microscopy; see Table 5 for details. (B) Iba1-positive microglia, (C) Brn3a-positive RGCs, and (D) peripapillary blood vessels in the choroid in intact eyes were clearly visible from the outside of the eyes. Scale bars, 100 µm.

CUBIC-1 treatment (Fig. 2B, Table 4). Tuj1 is an antibody against neuron-specific class III beta-tubulin and recognizes postmitotic neurons and axons. After washing, secondary antibody and propidium iodide were injected into the vitreous humor through the hole. After the entire immunostaining procedure, the eyes were incubated with CUBIC-2 reagent, and retinas were isolated and flat-mounted. We found many Tuj1-positive axons of RGCs running to the optic disc (Figs. 2C, 2D, lower panels). Similar staining patterns were obtained when isolated free-floating retinas were subjected to Tuj1 immunostaining (Figs. 2A, 2C, 2D, upper panels; Table 3). These results suggest that antibody injected into the vitreous humor recognized its antigen appropriately even after H_2O_2 and CUBIC-1 treatment. Consistent results were obtained using intact eyes of ICR mice and anti-Iba1 antibody, which is expressed in microglia. Iba1-positive microglia were clearly visualized by injecting anti-Iba1 antibody into the vitreous humor (Figs. 2E, 2F, lower panels). Taken together, our results indicate that antibody injection into the vitreous humor is effective and feasible for labeling specific proteins in intact eyes even after H_2O_2 and CUBIC treatment.

Imaging of the Retina from the Outside of Intact Mouse Eyes after Treatment with H_2O_2 and CUBIC, and Immunostaining

We next examined whether fluorescent signals in the retina can be visualized from the outside of the eye (Fig. 3A, Table 5). After the eyes of the adult C57BL/6J mice were treated with H_2O_2 and CUBIC-1 reagent, a solution containing anti-Iba1 antibody was injected into the vitreous humor through small holes made at the ora serrata. After washing, Alexa Fluor 488-conjugated secondary antibody (Thermo Fisher Scientific; Waltham, MA) and propidium iodide were injected into the vitreous humor through the hole. After the entire immunostaining procedure, eyes were incubated with CUBIC-2 reagent. Images of the retina were taken from the outside of the eye using a confocal microscope (LSM 5 Pascal laser scanning microscope, Plan-Apochromat 20×/0.8, Plan-Neofluar 10×/0.30; Carl Zeiss) without dissection of the eye. We found that Iba1-positive microglia in the retina were clearly observed from the outside of intact eyes (Fig. 3B). Consistently, clear images of Brn3a-positive RGCs were acquired using the same procedure

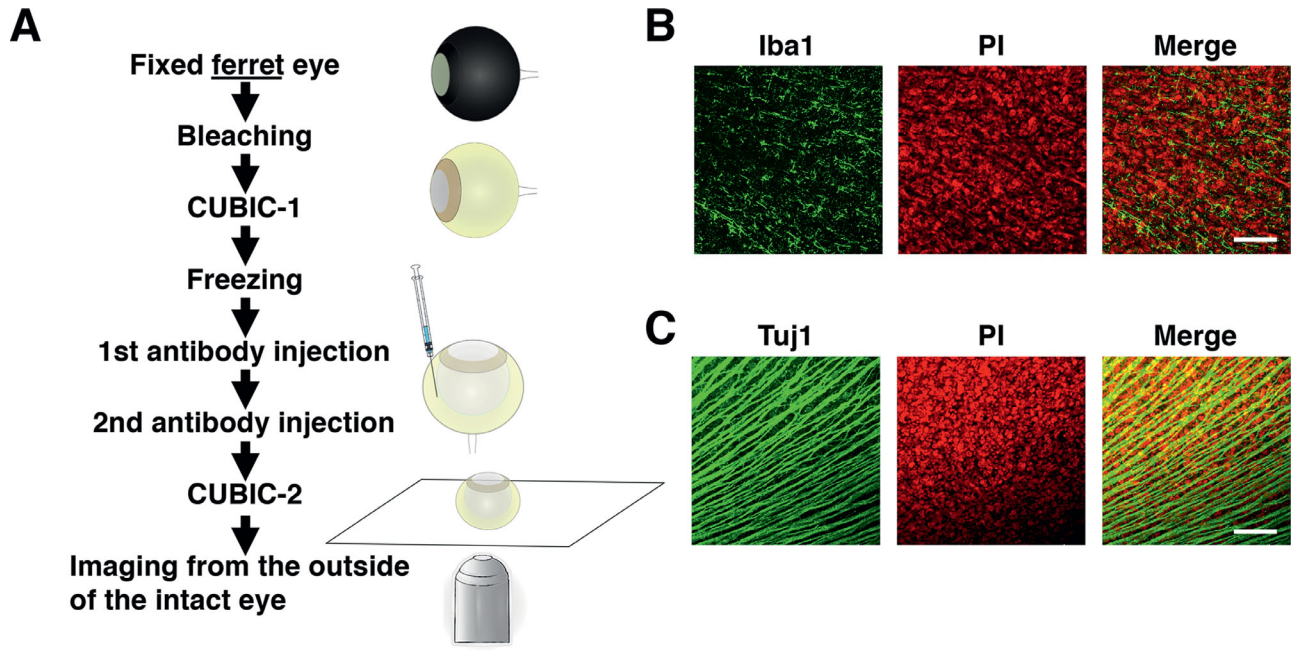

Figure 4. Imaging of the retina in intact ferret eyes from the outside of the eye. (A) Experimental procedure. After immunostaining using intact ferret eyes, images were taken from the outside of the eye without making sections using confocal microscopy; see Table 5 for details. (B) Iba1-positive microglia and (C) Tuj1-positive RGC axons in the intact ferret eyes were clearly visible from the outside of the eyes. Scale bars, 100 µm.

Table 5. Detailed experimental procedure for Figures 3 and 4

Day	Procedure
1	Cardiac perfusion with 4% PFA
	Isolation of the eye
	Post-fixation in 4% PFA at 4°C overnight
2	Washing with PBS, 10 min × 3
	Bleaching with 10% H_2O_2 for 3 h at 55°C
	Washing with PBS, 10 min × 3
	CUBIC-1 at RT for 1 d
3	Washing with PBS, 10 min × 3
	20% sucrose at 4°C for 1 d
	Freezing in OCT at –80°C overnight
4	Washing with PBS, 10 min × 3
	Blocking with 0.1% Triton X-100, 0.5% BSA at RT for 4 h
	First antibody injection and incubation at RT for 3 d
7	Washing with PBST, 10 min × 3
	Second antibody injection and incubation at RT for 1 d
8	Washing with PBST, 10 min × 3
	20% sucrose at 4°C for 1 d
9	CUBIC-2 at RT for 2 d
11	Imaging of the intact eye using a confocal microscope

BSA, bovine serum albumin; PBST, 0.5% Triton X-100/PBS; RT, room temperature.

(Fig. 3C). Furthermore, we performed the same procedure with anti-CD31 antibody and found that peripapillary blood vessels in the choroid were clearly stained (Fig. 3D). These results indicate that our method is useful for investigating the molecular and structural features of the retina from the outside of the eye of the adult C57BL/6J mouse.

Imaging of the Retina from the Outside of Intact Ferret Eyes after Treatment with H_2O_2 and CUBIC, and Immunostaining

Finally, we examined if our method is also applicable to the eyes of ferrets. We applied the same protocol to adult ferret eyes (Fig. 4A, Table 5). Confocal microscopies uncovered that Iba1-positive microglia and Tuj1-positive axons of RGCs in the retina were clearly visible from the outside of the eye (Figs. 4B, 4C), even though the size of the ferret eye is larger than that of the mouse eye. Thus, it seems plausible that our method is applicable to the eyes of various kinds of animals.

Discussion

Although many tissue clearing methods have been applied to various organs, tissue clearing methods

for the eye have not been established. Here, we combined CUBIC, which is a tissue clearing method involving removing lipid and reducing the refractive index of organs, with melanin bleaching using H_2O_2. We succeeded in making the intact eyes of mice and ferrets transparent, preserving fluorescence and tissue architectures. By using different kinds of antibodies, it was possible to visualize the distribution patterns and morphologies of various cell types in intact eyes. Our rapid and simple method opens the possibility of mapping various structures and functions in the eye without making tissue sections.

It should be noted that the retina can be damaged during our procedure, especially when small holes are made at the ora serrata, and solutions are injected into the vitreous humor. Careful intravitreal injection is a key step for preserving the retinal structures. Care should be taken not to damage the retina with injection needles. After bleaching and cleaning, the eye becomes more fragile. In this study, we tried various temperatures and incubation times for H_2O_2 treatment, and 10% H_2O_2 at 55°C for 3 hours seemed to be optimal. Longer incubation times, higher concentrations, and higher temperatures may affect immunoreactivity and structures of the eye.

Although we used normal eyes in this study, our method should also be powerful for investigating the pathophysiological mechanisms of various eye diseases. In glaucoma, for example, the axons of RGCs are damaged by high intraocular pressure.[23,24] Using glaucoma model mice and ferrets,[25–27] axonal damage in the intact eye can be examined with our method. Furthermore, a relationship between myopia and glaucoma has been proposed, as myopic eyes have an increased risk of glaucoma.[28] Optic nerve head changes such as tilt and torsion are associated with the progression of myopia and may in turn predispose toward glaucoma. However, because of the complexity of the interaction between them, the causative relationship between myopia and glaucoma remains to be further clarified.[29] Mouse models of experimental myopia showing elongation of the post-equatorial segment of the eye, as is the case in human myopia, have been developed.[30,31] Our method seems useful for investigating myopia-induced changes from the retina to the sclera at both molecular and macroscopic levels simultaneously in a whole-eye preparation. In addition to lowering eye pressure, new treatments directed at the retina and the brain could be developed.[32] It seems plausible that our method could be used to evaluate the effects of new treatments. In addition, our method should also be applicable to tumors. Previously, tissue clearing methods were used to visualize the brain microvasculature and the routes of the invasion of glioblastoma cells.[33] Quantitative analyses of the topographical relationship between glioblastoma cells and their microenvironment were performed. It would be intriguing to combine our method with mouse models of ocular tumors, and it would be important to investigate the extent to which our method could be used for visualizing tissues in tumors.

During the preparation of our manuscript, a pioneering study reported a tissue clearing method for the eye that combined melanin bleaching and the iDISCO tissue clearing method.[34] Although this report visualized the distribution patterns of vessels and S-opsin, it was unclear whether tissue clearing methods could be applied to various kinds of cells and structures in the retina. In addition, it was also unclear whether tissue clearing methods could be applicable to larger eyes from other animals. Our study using melanin bleaching and CUBIC demonstrated that the distribution patterns and morphology of microglia, RGCs, and RGC axons in the intact eye can be investigated from the outside of the intact eyes. Furthermore, our study indicates that our method is applicable not only to the eyes of mice but also to the larger eyes of ferrets. Visualization of retinal structures in the intact eye by combining melanin bleaching, tissue clearing, and immunostaining would provide a new avenue for investigating the functions of the retina and pathophysiological mechanisms of various eye diseases.

Acknowledgments

We thank Zachary Blalock and Kawasaki lab members for their helpful support.

Supported by Grants-in-Aid for Scientific Research from the Ministry of Education, Culture, Sports, Science and Technology; Japan Agency for Medical Research and Development; Daiichi Sankyo Foundation of Life Science; Kawano Masanori Memorial Public Interest Incorporated Foundation for Promotion of Pediatrics; Mitsubishi Foundation; Takeda Science Foundation; Kanazawa University SAKIGAKE project 2018; and Kanazawa University CHOZEN project.

Disclosure: **Y. Ye,** None; **T.A. Dinh Duong,** None; **K. Saito,** None; **Y. Shinmyo,** None; **Y. Ichikawa,** None; **T. Higashide,** None; **K. Kagami,** None; **H. Fujiwara,** None; **K. Sugiyama,** None; **H. Kawasaki,** None

References

1. Levin LA. Retinal ganglion cells and neuroprotection for glaucoma. *Surv Ophthalmol*. 2003;48:S21–S24.
2. Bringmann A, Pannicke T, Grosche J, et al. Müller cells in the healthy and diseased retina. *Prog Retin Eye Res*. 2006;25:397–424.
3. Almasieh M, Wilson AM, Morquette B, Vargas JLC, Di Polo A. The molecular basis of retinal ganglion cell death in glaucoma. *Prog Retin Eye Res*. 2012;31:152–181.
4. Hama H, Kurokawa H, Kawano H, et al. Scale: a chemical approach for fluorescence imaging and reconstruction of transparent mouse brain. *Nat Neurosci*. 2011;14:1481–1488.
5. Ke MT, Fujimoto S, Imai T. SeeDB: a simple and morphology-preserving optical clearing agent for neuronal circuit reconstruction. *Nat Neurosci*. 2013;16:1154–1161.
6. Tomer R, Ye L, Hsueh B, Deisseroth K. Advanced CLARITY for rapid and high-resolution imaging of intact tissues. *Nat Protoc*. 2014;9:1682–1697.
7. Ertürk A, Becker K, Jährling N, et al. Three-dimensional imaging of solvent-cleared organs using 3DISCO. *Nat Protoc*. 2012;7:1983–1995.
8. Kuwajima T, Sitko AA, Bhansali P, Jurgens C, Guido W, Mason C. ClearT: a detergent-and solvent-free clearing method for neuronal and non-neuronal tissue. *Development*. 2013;140:1364–1368.
9. Susaki EA, Tainaka K, Perrin D, et al. Whole-brain imaging with single-cell resolution using chemical cocktails and computational analysis. *Cell*. 2014;157:726–739.
10. Chung K, Wallace J, Kim SY, et al. Structural and molecular interrogation of intact biological systems. *Nature*. 2013;497:332–337.
11. Chung K, Deisseroth K. CLARITY for mapping the nervous system. *Nat Methods*. 2013;10:508–513.
12. Lee E, Kim HJ, Sun W. See-through technology for biological tissue: 3-dimensional visualization of macromolecules. *Int Neurourol J*. 2016;20:S15–S22.
13. Xu J, Ma Y, Yu T, Zhu D. Quantitative assessment of optical clearing methods in various intact mouse organs. *J Biophotonics*. 2019;12:e201800134.
14. Kagami K, Shinmyo Y, Ono M, Kawasaki H, Fujiwara H. Three-dimensional visualization of intrauterine conceptus through the uterine wall by tissue clearing method. *Sci Rep*. 2017;7:5964.
15. Kagami K, Shinmyo Y, Ono M, Kawasaki H, Fujiwara H. Three-dimensional evaluation of murine ovarian follicles using a modified CUBIC tissue clearing method. *Reprod Biol Endocrinol*. 2018;16:72.
16. Hohberger B, Baumgart C, Bergua A. Optical clearing of the eye using the See Deep Brain technique. *Eye (Lond)*. 2017;31:1496–1502.
17. Kawasaki H, Crowley JC, Livesey FJ, Katz LC. Molecular organization of the ferret visual thalamus. *J Neurosci*. 2004;24:9962–9970.
18. Iwai L, Kawasaki H. Molecular development of the lateral geniculate nucleus in the absence of retinal waves during the time of retinal axon eye-specific segregation. *Neuroscience*. 2009;159:1326–1337.
19. Iwai L, Ohashi Y, Van Der List D, Usrey WM, Miyashita Y, Kawasaki H. FoxP2 is a parvocellular-specific transcription factor in the visual thalamus of monkeys and ferrets. *Cereb Cortex*. 2012;23:2204–2212.
20. Sato C, Iwai-Takekoshi L, Ichikawa Y, Kawasaki H. Cell type-specific expression of FoxP2 in the ferret and mouse retina. *Neurosci Res*. 2017;117:1–13.
21. Kim SY, Assawachananont J. A new method to visualize the intact subretina from retinal pigment epithelium to retinal tissue in whole mount of pigmented mouse eyes. *Transl Vis Sci Technol*. 2016;5:6.
22. Richardson DS, Lichtman JW. Clarifying tissue clearing. *Cell*. 2015;162:246–257.
23. Quigley HA, Nickells RW, Kerrigan LA, Pease ME, Thibault DJ, Zack DJ. Retinal ganglion cell death in experimental glaucoma and after axotomy occurs by apoptosis. *Invest Ophthalmol Vis Sci*. 1995;36:774–786.
24. Chang EE, Goldberg JL. Glaucoma 2.0: neuroprotection, neuroregeneration, neuroenhancement. *Ophthalmology*. 2012;119:979–986.
25. Fujishiro T, Kawasaki H, Aihara M, et al. Establishment of an experimental ferret ocular hypertension model for the analysis of central visual pathway damage. *Sci Rep*. 2014;4:6501.
26. Johnson TV, Tomarev SI. Rodent models of glaucoma. *Brain Res Bull*. 2010;81:349–358.
27. Bouhenni RA, Dunmire J, Sewell A, Edward DP. Animal models of glaucoma. *J Biomed Biotechnol*. 2012;2012:692609.
28. Mitchell P, Hourihan F, Sandbach J, Wang JJ. The relationship between glaucoma and myopia:

the Blue Mountains Eye Study. *Ophthalmology*. 1999;106:2010–2015.
29. Tan NY, Sng CC, Ang M. Myopic optic disc changes and its role in glaucoma. *Curr Opin Ophthalmol*. 2019;30:89–96.
30. Tkatchenko TV, Shen Y, Tkatchenko AV. Mouse experimental myopia has features of primate myopia. *Invest Ophthalmol Vis Sci*. 2010;51:1297–1303.
31. Jiang X, Kurihara T, Kunimi H, et al. A highly efficient murine model of experimental myopia. *Sci Rep*. 2018;8:2026.
32. Weinreb RN, Aung T, Medeiros FA. The pathophysiology and treatment of glaucoma: a review. *JAMA*. 2014;311:1901–1911.
33. Lagerweij T, Dusoswa SA, Negrean A, et al. Optical clearing and fluorescence deep-tissue imaging for 3D quantitative analysis of the brain tumor microenvironment. *Angiogenesis*. 2017;20:533–546.
34. Henning Y, Osadnik C, Malkemper EP. EyeCi: optical clearing and imaging of immunolabeled mouse eyes using light-sheet fluorescence microscopy. *Exp Eye Res*. 2019;180:137–145.